Low-Impedance VHF and UHF Capacitive Silicon Bulk Acoustic-Wave Resonators—Part II: Measurement and Characterization

Siavash Pourkamali, *Member, IEEE*, Gavin K. Ho, *Student Member, IEEE*, and Farrokh Ayazi, *Senior Member, IEEE*

***Abstract*—In this part of the paper, extensive measurement results on the resonance, frequency tuning, and temperature characteristics of the silicon bulk acoustic-wave resonators (SiBARs) that were described in Part I will be presented and justified.**

***Index Terms*—Bulk acoustic wave resonators, high-aspect-ratio polysilicon and single-crystal silicon (HARPSS), MEMS, micromachining, micromechanical resonators, silicon resonators.**

I. Fundamental Mode Operation

A. Two-Port Resonators

THE FABRICATED two-port high-aspect-ratio polysilicon and single-crystal silicon (HARPSS)-on-silicon-on-insulator (SOI) silicon bulk acoustic-wave resonators (SiBARs) were tested in both vacuum and atmosphere using the test setup that was described in Part I. Fig. 1 shows the measured frequency response for a 300-μm-long 50-μm-wide 20-μm-thick SiBAR. A very clear resonance peak was observed for this resonator by applying polarization voltages of as low as 7 V [Fig. 1(a)]. A quality factor of 77 000 in vacuum and 24 400 in air were measured for the fundamental width-extensional bulk mode of this resonator at 85.9 MHz. Polarization voltages of up to 60 V were applied to the resonator, resulting in a total measured impedance of 680 Ω [Fig. 1(b)]. However, the quality factor of the resonator was gradually reduced to 22 500 by increasing the polarization voltage to 60 V. Gradual reduction of the measured quality factor is a result of the existence of a parasitic resistance R_{load} in series with the resonator motional resistance that loads the intrinsic mechanical Q of the resonator. From (3) in Part I, we have

$$Q_{\text{loaded}} = Q_{\text{unloaded}} \frac{R_m}{R_m + R_{\text{load}}} \tag{1}$$

where R_m is the motional resistance of the resonator, and Q_{unloaded} is the intrinsic mechanical Q of the resonator and is equal to the measured resonator quality factor at low polarization voltage before Q degradation starts. As the impedance of the resonator decreases by increasing the polarization voltage, the effect of the loading resistor on the quality factor becomes more pronounced [as confirmed by (1)].

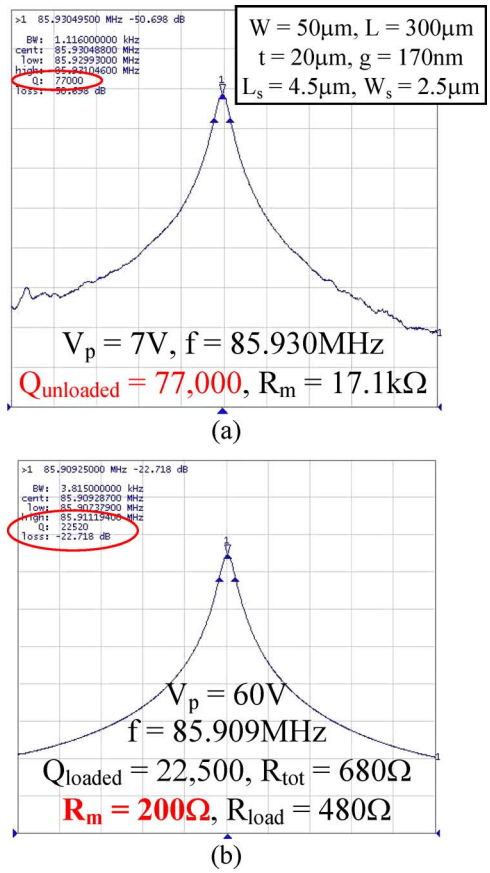

Fig. 1. Measured frequency response of a low-impedance 86-MHz SiBAR with (a) low and (b) high polarization voltages showing Q loading that is caused by the parasitic series resistance due to its very low motional resistance.

Using (1) and the fact that the total resistance that is computed based on the measured insertion loss at high V_p [using (4) in Part I] is the sum of the motional resistance of the resonator and the associated parasitic series resistance ($R_{\text{tot}} = R_m + R_{\text{load}}$), the value of the loading resistance and intrinsic motional resistance of the resonator can be calculated (two equations and two unknowns). For the resonator of Fig. 1, the extracted motional resistance is only 200 Ω, and the related parasitic loading resistance is 480 Ω.

For SiBARs that were fabricated in the previous work [1], support lengths were set to the quarter acoustic wavelength

Manuscript received October 11, 2006; revised March 29, 2007. The review of this paper was arranged by Editor K. Najafi.

S. Pourkamali is with the Department of Electrical and Computer Engineering, University of Denver, Denver, CO 80208 USA.

G. K. Ho and F. Ayazi are with the School of Electrical and Computer Engineering, Georgia Institute of Technology, Atlanta, GA 30332-0250 USA (e-mail: ayazi@ece.gatech.edu).

Color versions of one or more of the figures in this paper are available online at http://ieeexplore.ieee.org.

Digital Object Identifier 10.1109/TED.2007.901405

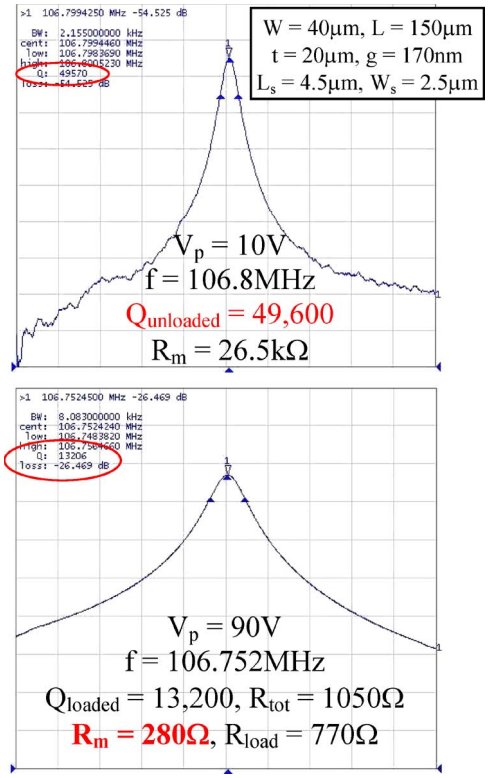

Fig. 2. Measured frequency response of a 106.8 MHz SiBAR with different polarization voltages.

at the frequency of their first width extensional mode, which is equal to half of the width of the SiBAR. For such support length, the resonance frequency for the extensional resonance mode of the support beam will be close to the resonance frequency of the SiBAR. Therefore, during operation of the resonator, the support beam will vibrate in its longitudinal mode, isolating any perpendicular displacement at the supporting point (displacement along the SiBAR length) from the substrate. Based on this argument [2], the quarter-wavelength supports were expected to reduce the support loss and improve the quality factor of the resonators significantly. However, measurement results of SiBARs revealed that resonators with quarter-wavelength supports do not have noticeably larger quality factors compared to the SiBARs in this paper with short (with a length of 3–5 μm) supports. On the other hand, much lower impedances can be achieved for the resonators with short supports. Short supports increase the stiffness of the resonator structure significantly, making it much more resilient against electrostatic pull-in or stiction during hydrofluoric acid release (as the gap sizes become smaller). Therefore, such resonators can tolerate much higher polarization voltages (or smaller gap sizes) and provide lower impedances. From the manufacturability and reliability points of view, having stiffer structures is also beneficial for improving shock resistance and long-term durability of the resonators.

Fig. 2 shows another example of a low-impedance 106.8 MHz (40 μm wide, 150 μm long, and 20 μm thick) SiBAR whose quality factor is being loaded by the series parasitic resistance. The quality factor for this resonator decreases from 49 600 to 13 200 by increasing the polarization voltage from 10 to 90 V, which is a result of existence of a 770 Ω loading resistance in series with the 280 Ω intrinsic motional resistance of the resonator (at $V_p = 90$ V). The extracted motional resistances on the order of 200 Ω are among the lowest impedance values that are reported for the HF air-gap capacitive resonators so far and are well within the desired range for RF circuit design applications.

B. Parasitic Resistance and Q Loading

To achieve lower overall resistances and eliminate Q loading as much as possible, it is important to have good understanding of the cause of the parasitic series resistance and its reduction or elimination.

The typical values of loading resistances for the fabricated resonators in this batch are in the range of 400–1000 Ω. The measured static resistances between the two polarization-voltage pads on the two ends of the SiBARs are close to the extracted loading resistor values. Therefore, the resistivity of the silicon structure in the V_p path is suspected to be responsible for Q loading.

The 50-Ω terminations of the network analyzer (a total of 100 Ω) constitute a portion of the parasitic series resistance, and the rest is blamed on the resistivity of the silicon structure of the resonator itself. For a SiBAR operating in its fundamental (or an odd) width-extensional mode, the displacement of the resonator body toward the electrodes on its two sides is in phase; therefore, in each cycle, charges from the polarization-voltage dc source have to pass back and forth through the resonator body. As a result, the physical resistance of the resonator body will act as a resistance in the path of the ac current passing through the resonator and will result in quality factor loading. This effect has also been previously observed and demonstrated in silicon carbide (SiC) capacitive microresonators due to their large substrate resistivity compared to silicon [3].

The immediate solution to this problem would be to fabricate the resonators on a silicon substrate with lower resistivity to reduce the resulting loading resistance. The starting SOI substrate for the resonators in Figs. 1 and 2 had a device layer resistivity of 0.015 $\Omega \cdot$ cm. To further verify this assumption and investigate the effect of substrate resistivity on Q loading, another batch of resonators was fabricated on an SOI substrate with lower device layer resistivity (0.002 $\Omega \cdot$ cm). Fig. 3 shows the frequency response and extracted resistance values for a 20-μm-thick 40-μm-wide 300-μm-long SiBAR with 125-nm capacitive gaps (Gap aspect ratio = 160) that are fabricated on the lower resistivity substrate.

The total extracted loading resistance for this resonator is only 120 Ω. Taking the 100-Ω loading that is caused by the 50-Ω terminations of the network analyzer into account, the remaining parasitic resistance that is blamed on the silicon structure is only 20 Ω, which is over an order of magnitude lower than the loading resistor for the devices on the previous higher resistivity substrate.

Second-order effects such as partial depletion that is induced in the silicon structure by the electrodes (or vice versa), changing its effective resistivity, can also be among other contributing factors to the Q loading. Due to extremely small vibration

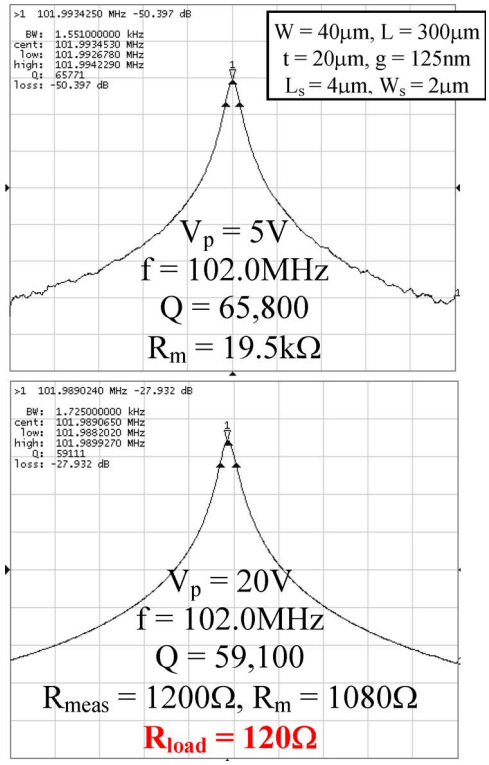

Fig. 3. Frequency response of a SiBAR with similar dimensions as the resonator of Fig. 2, which is fabricated on a lower resistivity substrate showing a much lower loading resistance of 120 Ω (with 20 Ω believed to be coming from the silicon structure).

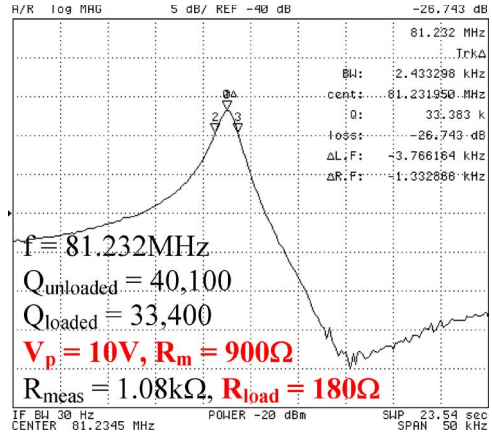

Fig. 4. Measured frequency response for a 30-μm-thick 50-μm-wide 540-μm-long SiBAR with 65-nm gaps.

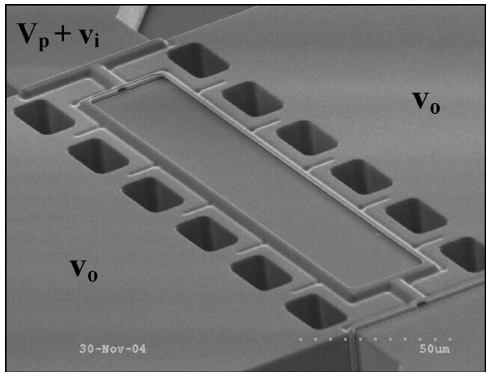

Fig. 5. SEM view of a 30-μm-wide 150-μm-long 20-μm-thick one-port SiBAR with 160-nm capacitive gaps. Polysilicon connecting the electrodes on the two sides covers the quarter-wavelength support beams.

amplitudes ($\sim$1 nm) of the bulk-mode resonators [4], mechanical nonlinearities are not believed to be involved.

The alternative approach for relaxation of the Q-loading issue is using other resonance modes of operation for the resonators, as demonstrated in [3], so that charges will not have to flow through the V_p path in each cycle and will only transfer from one side of the resonator to its other side (experiencing less structural resistance). For the SiBAR structures that are discussed in this paper, this can be achieved by the operation of the resonators in their second (or any even) width-extensional resonance mode.

C. Low-V_p Operation

With the resonator gap sizes in the range of 100–200 nm, as the ones in Figs. 1–3, comparatively large polarization voltages are required to achieve impedance values in the sub-kiloOhm range. By reduction of the capacitive gaps to 100 nm and below, the required polarization voltages can be significantly reduced. The alternative solution would be increasing the thickness and length of the resonators to increase the transduction area. Fig. 4 shows the measured frequency response for a 30-μm-thick SiBAR (540 μm long and 50 μm wide) with 65-nm capacitive gaps (a gap aspect ratio of $\sim$460, which is the highest demonstrated using HARPSS to date).

Due to the smaller gap size and larger length and thickness for this resonator, sub-kiloOhm motional resistances can be achieved with polarization voltages of as low as 10 V. Such dc bias voltages can be generated and controlled on a CMOS chip [5], [6].

D. One-Port Resonators

For some of the fabricated resonators, the electrode layout was slightly modified, so that the electrodes on the two sides of the SiBAR are electrically connected by the pad polysilicon. Fig. 5 shows the scanning electron microscope (SEM) view of a 30-μm-wide 150-μm-long 20-μm-thick one-port SiBAR. Polysilicon bridging over the support beams connects the electrodes on the two sides.

Such resonators have to be operated in one-port configuration. In a one-port configuration, the input ac signal v_i and the dc bias voltage V_p are applied to the body of the resonator, and the output signal is collected from the electrodes by direct connection to the network analyzer. A large bias resistor and a dc-block capacitor are used to isolate the ac and dc signals at the input.

For one-port resonators, the electrode–resonator capacitance, which is on the order of hundreds of femtofarads, acts as a feedthrough capacitance between the input and output nodes. The main advantage of two-port resonators is their lower feedthrough capacitance. For a two-port SiBAR with input and output electrodes on the two sides of the resonator, there is

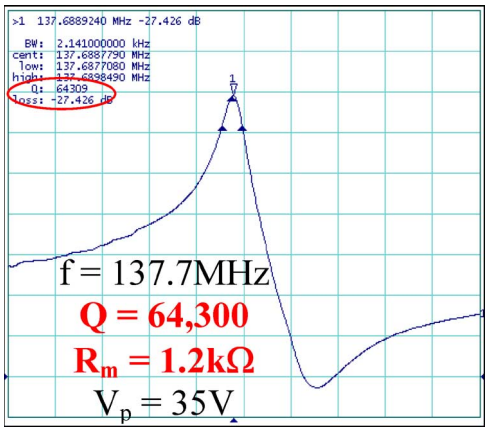

Fig. 6. Frequency response of the SiBAR of Fig. 5 measured in a one-port configuration.

almost no direct capacitive path from input to output. The body of the resonator, which is an ac ground, isolates the input and output signals, and only fringing capacitances that are on the order of a few femtofarads act as capacitive feedthrough for such devices. On the other hand, since the electrode area is divided into two separate sections for sensing and actuation, the effective electrode area for two-port resonators is half of that of a one-port resonator. This results in four times larger equivalent impedance for the two-port resonators. In conclusion, for applications where capacitive feedthrough can be tolerated to some extent, one-port-configured resonators providing four times lower impedances are a better choice.

Fig. 6 shows the measured frequency response of the one-port SiBAR of Fig. 5. The resonator was operated in its first horizontal thickness mode at 137.7 MHz and demonstrated a comparatively high quality factor of 64 300 in vacuum. Impedances of as low as 1.2 kΩ were measured for this resonator, while for the two-port resonators with similar dimensions (long support beams), the lowest measured impedances are in the range of 5–7 kΩ.

It is worth mentioning that the antiresonance peaks that are observed in Fig. 6 and some of the other frequency response plots are a result of parallel resonance of the resonator with its feedthrough capacitance. The calibration that is performed for the measurements should ideally eliminate the feedthrough capacitances; therefore, antiresonance peaks are not observed in most of the plots (although all resonators have some feedthrough capacitance). However, if the calibration is not 100% accurate at the time of measurement, a small portion of the feedthrough capacitance will affect the response by causing the antiresonance peaks. As long as the feedthrough level (out-of-band transmission) is ∼10–20 dB lower than the resonance peak Q, the resonance frequency and impedance measurements will have adequate accuracy.

II. Operation in Higher Resonance Modes

Operation of resonators in their higher resonance modes is a good approach to achieve higher resonance frequencies without pushing the resonator dimensions into ranges that are challenging to fabricate accurately. Using the higher order resonance

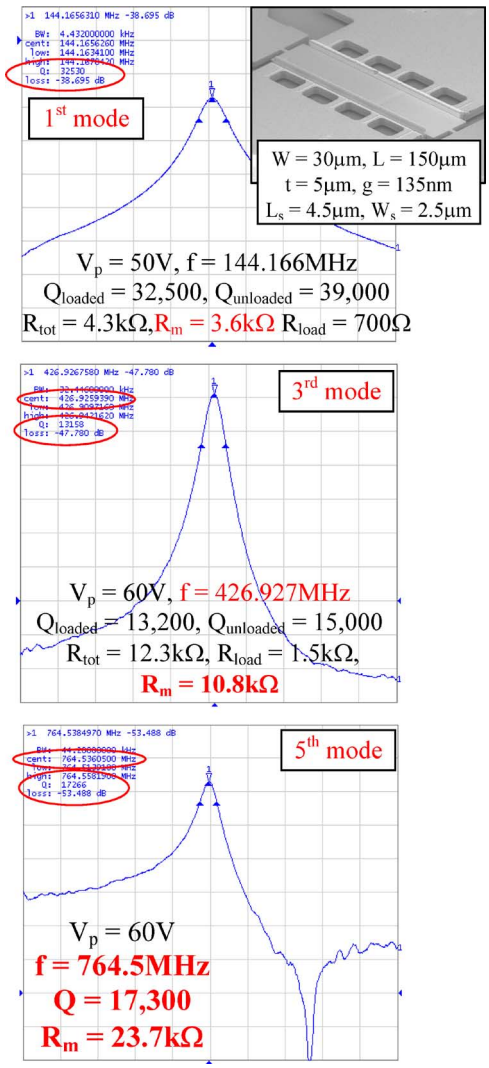

Fig. 7. Measured frequency response of a 30-μm-wide 150-μm-long 5-μm-thick SiBAR operating in its first and higher odd resonance modes up to the fifth mode.

modes eases the requirement on the tolerance of the resonator size variations (that are inevitable in high-volume manufacturing). On the other hand, resonator equivalent stiffness for higher resonance modes is larger than the fundamental mode and will add to the impedance issues for capacitive resonators.

The support beams for the SiBARs in this paper are placed in the middle of the resonator width. Therefore, in the even-width extensional modes, the supports will be subject to a large vibration amplitude that is imposed by the resonator and will introduce excessive energy loss to the substrate. This results in lower quality factors for such modes. However, for the odd higher order width-extensional modes, similar to the first mode, the midpoint of the device width is still the resonance node (i.e., has close-to-zero vibration amplitude), and high quality factors can be obtained.

Fig. 7 shows the measured frequency response of a 30-μm-wide 150-μm-long 5-μm-thick SiBAR operating in its first and higher odd width extensional modes up to the fifth mode. A quality factor of 17 300 at a resonance frequency of 765 MHz has been measured for the fifth mode of this resonator.

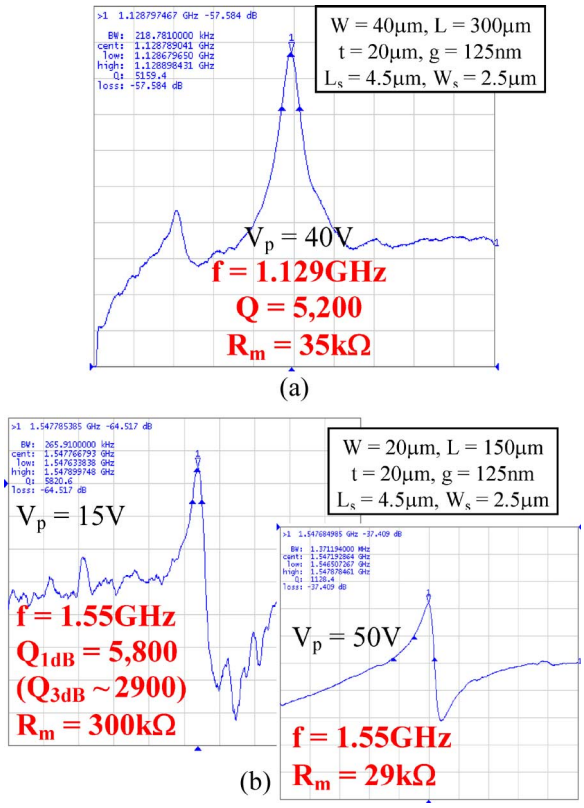

Fig. 8. Measured frequency responses for 20-μm-thick clamped–clamped SiBARs operating in their higher bulk modes with frequencies in excess of 1 GHz.

Impedance of as low as 23.7 kΩ was measured for this resonance mode, which is close to one order of magnitude lower than the typical reported motional resistance values for air gap capacitive resonators at such high frequencies [2], [7]. For the fifth resonance mode, as shown in Fig. 3 in Part I, the dimensions are in the range where severe mode shape distortion occurs. For such dimensions, the resonant frequency dependence on the resonator thickness becomes very sharp, and the resonance frequency can easily change by 10%–20% due to slight changes in the resonator thickness (Fig. 2 in Part I). Therefore, the comparatively large deviation between the measured and simulated frequencies for the fifth mode is due to sharp thickness dependence of the resonance frequency in this mode and uncertainties in the assumed resonator dimensions for modal analysis.

Fig. 8 shows the resonance peaks in the gigahertz frequency range that are measured for higher resonance modes of thick SiBARs. The plots are taken from 40- and 20-μm-wide SiBARs with expected first-mode resonance frequency of about 100 and 200 MHz, respectively. In Fig. 8(b), due to the comparatively large resistance of the resonator for such a high frequency, the resonant peak does not reach more than 3 dB above the feedthrough level; therefore, instead of the 3-dB Q, its 1-dB quality factor has been measured. Theoretically, for a second-order (LCR) resonator, the 1-dB bandwidth is half the 3-dB bandwidth, so $Q_{3\mathrm{dB}}$ is expected to be half the measured $Q_{1\mathrm{dB}}$. The effect of the large feedthrough has been taken into account in motional resistance calculations.

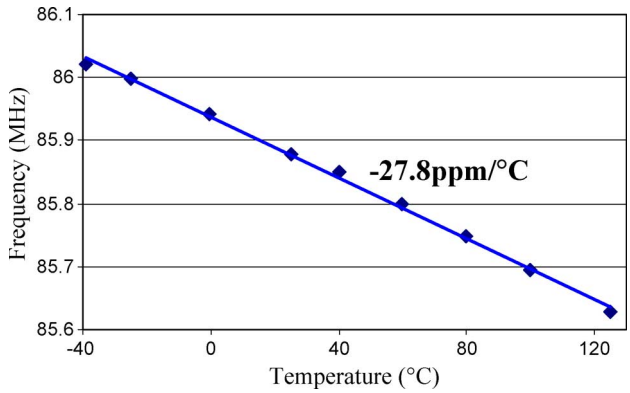

Fig. 9. Temperature dependence of frequency for a 540-μm-long 50-μm-wide 20-μm-thick (86 MHz) SiBAR showing a TCF of -27.8 ppm/°C.

Frequency-wise, the resonance peaks should correspond to the 11th and 7th width extensional modes of the structures; however, since the resonator thickness and length are much larger than the effective width for such modes, the mode shapes for such resonance modes are expected to be extremely wavy and distorted. Therefore, referring to them as higher width extensional modes does not seem to be appropriate. Finite-element analysis to find such mode shapes requires a large number of elements and results in a very large number of modes, which makes running the simulation and recognition of the right modes quite complicated and out of the scope of this paper.

Although hard to predict and analyze, such higher resonance modes are a promising approach to realize HF capacitive resonators (in the gigahertz range) with reasonable impedances. For instance, after experimental determination of some of the most suitable dimensions for maximized electromechanical coupling, one can scale the resonator dimensions up or down (while keeping the ratios the same), to generate a wide variety of different frequencies.

For the 40-μm-wide device, a very strong first resonance mode was detected at 102 MHz. However, for the 20-μm-wide resonator, since the resonator width and thickness are equal, a very weak (high impedance) first mode was detected at 170 MHz. This results from the inefficient coupling and excessive cancellation for this mode shape, which is completely expected (Fig. 2 of Part I). This can be very helpful when the resonator is desired to operate in its 1.55-GHz mode. The impedances that are measured for the HF modes are much smaller ($\sim$10$\times$) than that of the other reported values for air-gap capacitive resonators operating in the gigahertz range [2], [7].

III. Temperature Characteristics and Compensation

The other major bottleneck that limits the performance of capacitive SiBARs as frequency references for some of the high-precision applications is their much larger temperature coefficient of frequency (TCF) compared to quartz resonators. Fig. 9 shows the measured temperature dependence of resonant frequency for an 86-MHz SiBAR over the temperature range

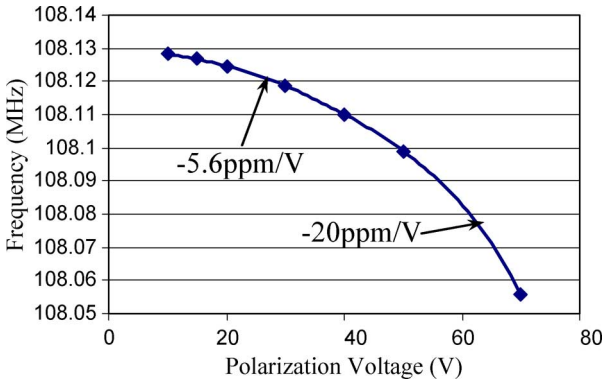

Fig. 10. Measured electrostatic tuning characteristic of a 108-MHz SiBAR showing a tuning range of over 70 kHz.

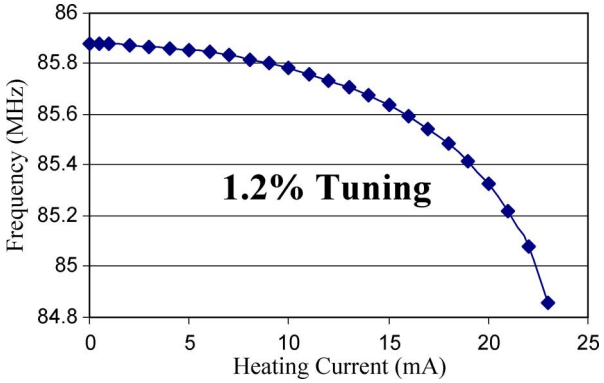

Fig. 11. Heat-induced tuning characteristic of the 86-MHz SiBAR of Fig. 9 by passing current through the body of the resonator.

of -40°C to 120°C. The temperature sensitivity that is shown in Fig. 9 has a linear behavior with a TCF of -27.8 ppm/°C, which is very close to that of single-crystal silicon disk resonators [4] and piezoelectric film bulk acoustic resonators [8], but more than ten times larger than typical quartz crystals. As shown in [4], the temperature sensitivity of silicon resonators is mainly due to the large temperature coefficient of the Young's modulus of silicon.

Electrostatic and heat-induced frequency tuning for temperature compensation of capacitive silicon resonators are briefly discussed here. Electrostatic tuning of parallel-plate capacitive resonators, which is well known and has been used for temperature compensation of lower frequency resonators [5], [6], is considered to be one of the most convenient and power-efficient temperature compensation techniques. However, for high frequency resonators with operating frequencies of hundreds of megahertz and higher, extremely large resonator stiffness (and consequently, its resonant frequency) can hardly be tuned by the V_p-induced electrical stiffness. Fig. 10 shows the measured electrostatic tuning characteristic for a 108-MHz SiBAR with 135-nm capacitive gaps. A frequency tuning of 70 kHz is demonstrated for this resonator by changing the polarization voltage from 10 to 70 V. The tuning slope for a capacitive SiBAR assuming a nondistorted mode shape is given by

$$\frac{\partial f}{\partial V_p} = -\frac{2V_p f \varepsilon A_e}{K g^3} \tag{2}$$

where f is the resonance frequency of the resonator, A_e is the electrode area (area of one electrode only), and K is the effective stiffness, as defined in (1) in Part I.

A tuning range of about 300 kHz is required to compensate a 108-MHz resonator over a 100 °C temperature range. According to (2), such tuning range can be achieved by reduction of the capacitive gap sizes to 70 nm and changing the polarization voltage over a range of 5–40 V, which seems to be possible although challenging. However, as the frequency increases, the required electrical stiffness for temperature compensation increases proportionally, making it even more challenging. In addition, changing the polarization voltage of the resonator changes its equivalent electrical impedance significantly, which is not desirable from the circuit-design point of view. The solution to this problem would be to split the electrodes around the resonator into two electrically isolated sections: 1) one for electrostatic transduction (sense and drive) and 2) one for frequency tuning. In this case, a smaller electrode area for each mechanism will result in higher resonator impedance and lower electrostatic tuning (four times higher impedance and two times lower tuning in case of equally divided electrodes). Therefore, further pushing of the gap sizes to smaller values will be required.

The more effective but power-consuming approach that is examined here is tuning the resonance frequency of the resonator by passing an electrical current through its structure and consequently changing its temperature. Temperature compensation based on resonator Joule heating has been demonstrated in [9] and [10]. Since the SiBARs are supported by two support beams on the two sides, two polarization-voltage bonding pads are available on the two ends of the resonator. By applying slightly different dc voltages to the two pads on the two ends of the resonator, the dc current will pass through the SiBAR structure and elevate its temperature. Fig. 11 shows the frequency-tuning characteristic of the SiBAR of Fig. 9 by passing current through it. More than 1 MHz (1.2%) of frequency tuning has been achieved by passing up to 24 mA of dc current through the body of the resonator. According to the measured temperature-induced frequency drift (Fig. 9), this corresponds to an elevated temperature of up to 450 °C for the resonator. It is worth noting that the resonator was operating flawlessly, with no degradation of its quality factor at such high temperature.

This tuning technique can be deployed for temperature compensation of HF SiBARs [9], [10]. A temperature-dependent current source can be used to keep the temperature of the resonator elevated (e.g., at 125 °C), independent of the temperature of the surrounding environment, and avoid temperature-induced frequency shifts. In this case (unpackaged resonator on a 1.2×1.2 cm^2 silicon substrate with no thermal isolation from the test setup), 85 mW of power was required at room temperature to keep the temperature of the resonator elevated at 125 °C. This can be reduced to a few milliwatts or even below milliwatts for a single resonator inside a thermally isolated package. Furthermore, due to the dependence of the resistivity of the resonator structure to temperature, the resonator itself can be used simultaneously as a temperature sensor in the temperature control feedback loop.

IV. Conclusion

High frequency bulk-mode resonant structures referred to as "SiBAR" were presented as a strong and viable approach toward implementation of high-Q low-impedance HF capacitive resonators. Using the potentially unlimited capacitive transduction area that is provided through the combination of the HARPSS fabrication process and the SiBAR structures, impedances well in the required RF range can be achieved for such resonators in the very-high-frequency (VHF) and ultra-high-frequency (UHF) ranges. Preliminary measurement results for the capacitive SiBARs in the VHF range show motional resistances in the sub-kilo-Ohm to few kilo-Ohm range with quality factors as high as side-supported disk resonators (20 000–100 000). Resonant frequencies in the UHF range were demonstrated for higher bulk extensional modes of the SiBARs with much smaller motional resistances compared to the previously demonstrated air-gap capacitive resonators operating in the UHF band.

Although with current resonator dimensions and capacitive gap sizes, their performance in the UHF range is not as promising, it can be shown theoretically that the same specifications can be met at higher frequencies by proportional downscaling of all the dimensions (including the gap sizes) as well as the polarization voltage.

The silicon structures of SiBARs have two electrical connections on their two sides. This facilitates implementation of highly stable temperature compensated oscillators by employing such device as a heater and temperature sensor as well as frequency reference simultaneously.

References

[1] S. Pourkamali, G. K. Ho, and F. Ayazi, "Vertical capacitive SiBARs," in *Proc. MEMS*, 2005, pp. 211–214.

[2] S. Li *et al.*, "Micromechanical hollow disk ring resonators," in *Proc. MEMS*, 2004, pp. 821–824.

[3] S. Bhave, D. Gao, R. Maboudian, and R. T. Howe, "Fully-differential poly-SiC Lame mode resonator and checkerboard filter," in *Proc. MEMS*, 2005, pp. 223–226.

[4] S. Pourkamali *et al.*, "VHF single crystal silicon capacitive elliptic bulk-mode disk resonators—Part II: Implementation and characterization," *J. Microelectromech. Syst.*, vol. 13, no. 6, pp. 1054–1062, Dec. 2004.

[5] G. K. Ho *et al.*, "Low impedance, highly tunable, I2-resonators for temperature compensated reference oscillators," in *Proc. MEMS*, 2005, pp. 116–120.

[6] G. K. Ho *et al.*, "Temperature compensated IBAR reference oscillators," in *Proc. MEMS*, 2006, pp. 910–913.

[7] J. Wang, Z. Ren, and C. T.-C. Nguyen, "Self-aligned 1.14 GHz vibrating radial-mode disk resonators," in *Proc. Transducers*, 2003, pp. 947–950.

[8] J. D. Larson *et al.*, "Power handling and temperature coefficient studies in FBAR duplexers for the 1900 MHz PCS band," in *Proc. Ultrason. Symp.*, 2000, vol. 1, pp. 869–874.

[9] M. A. Hopcroft, M. Agarwal, K. K. Park, B. Kim, C. M. Jha, R. N. Candler, G. Yama, B. Murmann, and T. W. Kenny, "Temperature compensation of a MEMS resonator using quality factor as a thermometer," in *Proc. MEMS*, 2006, pp. 222–225.

[10] M. Hopcroft, R. Melamud, R. N. Candler, W.-T. Park, B. Kim, G. Yama, A. Partridge, M. Lutz, and T. W. Kenny, "Active temperature compensation for micromachined resonators," in *Proc. Solid State Sens. and Actuators Workshop*, Hilton Head Island, SC, 2004, pp. 364–367.

Siavash Pourkamali (S'02–M'06) received the B.S. degree in electrical engineering from Sharif University of Technology, Tehran, Iran, in 2001 and the M.S. and Ph.D. degrees from Georgia Institute of Technology, Atlanta, in 2004 and 2006, respectively.

He is currently an Assistant Professor in the Department of Electrical and Computer Engineering, University of Denver, Denver, CO. He is the holder of five patents in the areas of silicon micro/nanomechanical resonators and filters, and nanofabrication technologies. His main research interests are integrated silicon MEMS and microsystems, micromachining technologies, RF MEMS resonators and filters, nanomechanical resonant sensors, and micro/nanorobotics for cell and molecular biology.

Prof. Pourkamali was the recipient of the 2005 Georgia Tech Sigma Xi Best M.S. Thesis Award, a 2006 Georgia Tech Electrical and Computer Engineering Research Excellence Award, and a silver medal in the 29th International Chemistry Olympiad.

Gavin K. Ho (S'01) was born in Vancouver, BC, Canada. He received the M.Eng. and B.A.Sc. degrees [with distinction in mechanical engineering (electromechanical design option)] from the University of British Columbia, Canada in 2001. He is currently working toward the Ph.D. degree in the School of Electrical and Computer Engineering, Georgia Institute of Technology (Georgia Tech), Atlanta.

He then joined Georgia Tech, where he was given the opportunity to teach undergraduate courses. His primary teaching objectives include instilling curiosity in science and motivating interdisciplinary research. His research interests include capacitive and piezoelectric micromechanical resonators for sensors, reference oscillators, and bandpass filter applications.

Mr. Ho was the recipient of the UBC Letson Prize in 2001 and the Col. Oscar P. Cleaver Award and N. Walter Cox Fellowship from the School of Electrical and Computer Engineering, Georgia Tech.

Farrokh Ayazi (S'96–M'00–SM'05) received the B.S. degree from the University of Tehran, Tehran, Iran, in 1994 and the M.S. and Ph.D. degrees from the University of Michigan, Ann Arbor, in 1997 and 2000, respectively, all in electrical engineering.

He joined the faculty of Georgia Institute of Technology, Atlanta, in December 1999, where he is currently an Associate Professor in the School of Electrical and Computer Engineering. His research interests are integrated micro- and nanoelectromechanical resonators, IC design for MEMS and sensors, RF MEMS, inertial sensors, and microfabrication techniques.

Prof. Ayazi was the recipient of the National Science Foundation CAREER Award in 2004, the Richard M. Bass Outstanding Teacher Award (determined by the vote of the ECE senior class) in 2004, the Georgia Tech College of Engineering Cutting Edge Research Award for 2001–2002, and a Rackham Predoctoral Fellowship from the University of Michigan for 1998–1999. He is an Editor for the IEEE/ASME Journal of Microelectromechanical Systems and serves on the technical program committees of the IEEE International Solid-State Circuits Conference and the International Conference on Solid-State Sensors, Actuators and Microsystems (Transducers).